Self-powered Carbon Nanotube Yarn for Acceleration Sensor Application

Bum-Joon Kim, Yongwoo Jang, Ji Hwan Moon, Ray H. Baughman, and Seon Jeong Kim

***Abstract*—Accelerometers are indispensable for detecting accelerating forces in automotive electronic systems. Although several accelerometers have been developed, they are still unstable for vehicle dynamics applications in the low frequency range (0-20 Hz). Here, we report a novel type of accelerometer based on a coiled carbon nanotube (CNT) yarn as a self-powered and low frequency range-covered acceleration sensor. The proposed sensor is designed in a compact fiber-like structure for practical applications. Open circuit voltage (OCV) signals are consistently generated during the stretch-and-release process of the coiled CNT yarn by the applied sinusoidal accelerations, and the OCV changes increase linearly with increasing acceleration from 4.84 to 48.37 m/s^2. Our accelerometer exhibits excellent dynamic sensing performance in the low frequency range compared with commercial accelerometers. In an application as a CNT yarn device configured with a mass load, the OCV change is linearly proportional to the applied acceleration. When our accelerometer is attached to a seatbelt in a vehicle, it generates OCV changes from the movement of the body mass underlying a certain acceleration change. Given its excellent sensing performance, the CNT yarn acceleration sensor could be further developed for practical applications such as seatbelts and car seats with fabric and textile.**

***Index Terms*—acceleration, carbon nanotube, self-power, sensor, yarn**

I. Introduction

An accelerometer is an electromechanical device used to measure accelerating forces that have potential applications in various fields such as satellites, biomedical devices, mechanical structure testing, the automotive industry, and earthquake monitoring [1], [2]. In particular, automotive accelerometers have been used for electronic detecting systems such as crash detection, antilock braking, traction and suspension control, electronic steering, and chassis guidance [3]-[5]. Although a number of automotive accelerometers have been developed to date, they are still limited in stable detection at the low frequency range [6], [7]. For example, piezoelectric-type accelerometers are mostly applied as automotive sensors [8]-[10], but they exhibit sensitivity degradation at low-frequency ranges [11], [12].

Piezoelectric accelerometers require input power and an electric circuit for transducing into a voltage output. The input power consumes an external power source such as batteries and generates an electrical delay that causes a slow response time [13]. Recently, various types of self-powered acceleration sensors have been reported using nanogenerators based on triboelectric, piezoelectric, and pyroelectric materials [14]-[17]. However, their acceleration sensing performances were very poor compared with commercial accelerometers [18], [19]. Hence, for high-performance automotive vehicles, self-powered and low-frequency range-covered accelerometers are required.

Carbon nanotube (CNT) yarns made by twist insertion of a CNT sheet are known to exhibit excellent mechanical and electrical properties with a large porous surface area [20]-[22]. Previous studies have presented the feasibility of sensor applications of CNT yarns with respect to strain deformation, force variance, and human health monitoring [23]-[28]. Our group recently provided a CNT yarn harvester (referred to as "Twistron") that can convert mechanical energy into electrical energy without external bias voltage [29]. It was found that stretching a coiled CNT yarn generates an open-circuit voltage (OCV) and electrical power within 30 Hz of frequency in proportion to the strain deformation of the CNT yarn [29], [30].

Here, we demonstrate a self-powered and low frequency range-covered CNT yarn sensor as a novel type of accelerometer. The proposed accelerometer sensor was compactly designed and fabricated as a fiber-like single-body structure for practical applications. As a sensing electrode, the coiled CNT yarn was characterized under various conditions with different accelerations, displacements, and frequencies. In particular, we evaluated the acceleration sensing characteristics in the low frequency range (0–20 Hz) that are relevant to acceleration environments in automotive vehicles, and compared the performance with a commercial accelerometer. Furthermore, we showed the functional applications of a coiled CNT yarn as an accelerometer using a mass configured device and body mass.

Manuscript received August 9, 2019; revised December 13, 2019; accepted February 10, 2020. Date of publication Month xx, 2020; date of current version Month xx, 2020. This work was supported by the Creative Research Initiative Center for Self-Powered Actuation in the National Research Foundation of Korea (NRF).

Bum-Joon Kim, Yongwoo Jang, Ji Hwan Moon, and Seon Jeong Kim are with Center for Self-Powered Actuation and Department of Biomedical Engineering, Hanyang University, Seoul, 04763, South Korea (e-mail: bjkim82@hanyang.ac.kr; ywjang@hanyang.ac.kr; jhmoon95@hanyang.ac.kr; sjk@hanyang.ac.kr).

Ray H. Baughman is with The Alan G. MacDiarmid NanoTech Institute, The University of Texas at Dallas Richardson, TX 75080, USA (e-mail: Ray.Baughman@utdallas.edu).

II. SENSOR DESIGN

Fig. 1 illustrates a self-powered CNT yarn sensor that comprises a coiled CNT yarn as the working electrode, a ply of an untwisted CNT yarn as counter electrode, and a NaCl aqueous solution as an electrolyte connecting two electrodes, all of which are packed inside a silicone rubber tube. A coiled CNT yarn with self-coiled structure as the working electrode is fabricated by inserting twist using supporting load and microstructures such as yarn diameter, bias angle, coil pitch length, and intra-bundle porosity, which is associated with its electrochemical state, is sensitive to yarn length change by stretching and releasing [29]. By contrast, the counter electrode with a ply of uncoiled CNT yarns is insensitive to changes in yarn length due to the plied CNT yarn without twist insertion. Open-circuit voltage (OCV), electric voltage potential difference between two electrodes, generates as a sensor signal without input voltage. The acceleration causes stretching of the CNT yarn sensor, consequently, the CNT yarn sensor generates an OCV change as an output signal when accelerated. The principles of this yarn-type acceleration sensor are discussed in further detail below.

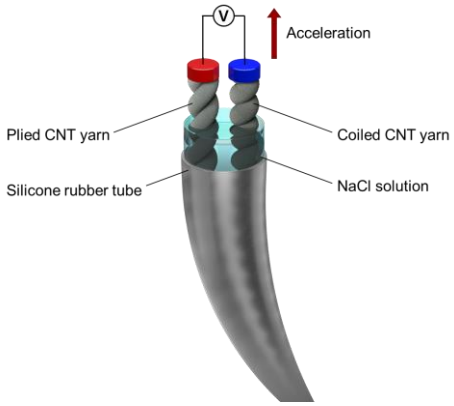

Fig. 1. Schematic diagram of self-powered CNT yarn acceleration sensor.

III. EXPERIMENTAL METHODS

A. Materials

Coiled and plied CNT yarns were fabricated by using a commercial CNT fiber (C-type, Murata Machinery, Ltd. Japan) made from multiwalled carbon nanotube (MWCNT) forests with a diameter of about 40 μm. NaCl (anhydrous, ACS reagent, ≥99%, Sigma Aldrich, USA) was used for the 0.6 M NaCl aqueous solution. The silicone rubber tube (Silicone Intravascular Tubing (Silastic®)), with inner and outer diameters of 1.0 and 2.2 mm, respectively, was purchased from Instech Laboratories, Inc, USA.

B. Fabrication of the CNT Yarn Sensor

The CNT yarn sensor consists of working/counter electrodes, electrolyte, and silicone tube packaging (Fig. 1). The working electrode was fabricated by coiling a four-ply CNT yarn, and a CNT coil with an average coil diameter of 125 μm, and a spring index of 0.45–0.47; the amount of twist insertion was 2,730 turns/m [31], [32]. The counter electrode was an uncoiled CNT yarn ply, and the length of both electrodes was 50 mm. All of the working/counter electrodes and the electrolyte (0.6 M NaCl aqueous solution) were packed in a silicone tube, and both sides of the electrodes were tethered.

C. Characterizations

Two-electrode experiments were conducted using coiled and plied CNT yarns as the working and counter electrodes, respectively [29]. The OCV, i.e., the potential difference between the working and the counter electrodes was measured using a digital oscilloscope (InfiniVision, model DSOX4024A, Keysight Technologies, USA). The applied acceleration was estimated from the yarn length variation, and calculated with second-order differentiation of all the data points of the dynamic yarn length changes by using mathematical software (Origin(Pro), Version 2016, OriginLab Corporation, USA).

Fig. 2 shows Acceleration sensing system setup for CNT yarn sensor. An electrodynamic vibration exciter (model 2007E, Modal Shop, Inc., USA) was used for periodic acceleration sensing characterization. The vibration exciter with the function generator generates sinusoidal tensile vibrations and the vibration component is directly connected with the CNT yarn and the commercial sensors. One side of the CNT yarn sensor was fixed tightly onto the vibration component and the other side was tethered on ground. The commercial acceleration sensor (model 8315A2D0, Kistler™, USA) was capacitive single axis accelerometer, the acceleration range was 0-98 m/s^2, in the low frequency range (0-200 Hz); the generated voltage output was Vout. The exciter vibration with variable frequency (1-20 Hz) at a constant strain (30%, 15 mm) was used to characterize the frequency response. A commercial acceleration sensor device was set by the vibration component. Three voltage output signals (the generated waveforms by the function generator, the CNT yarn, and the commercial sensors) were measured and recorded with digital oscilloscopes simultaneously.

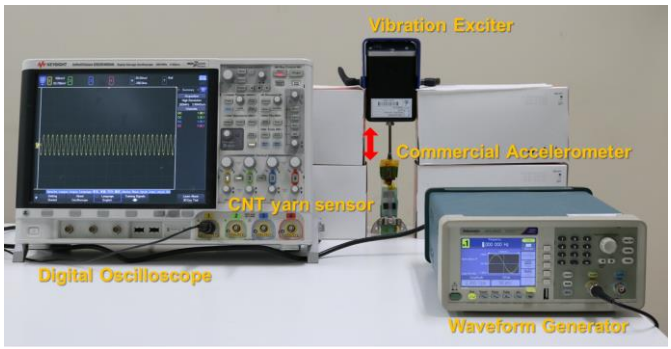

Fig. 2. Acceleration sensing system setup for CNT yarn and commercial sensors. Electrodynamic vibration exciter (Modal Shop, Inc. Model 2007E) with a function generator signal that generates sinusoidal tensile vibrations and the vibration component is directly connected with the CNT yarn and the commercial sensor. One side of the CNT yarn sensor was fixed tightly onto the vibration component and the other side was tethered on ground. The commercial acceleration sensor device was set by the vibration component.

IV. RESUTLS AND DISCUSSION

Fig. 3 shows the time-dependent OCV change of the coiled CNT yarn when accelerated. The OCV change generated was ~23.02 mV when the change in acceleration was 28.96 m/s^2 with 25% strain for 0.1 s. The blue line in Fig 3 represents the estimated acceleration from the variation in yarn length, calculated with second-order differentiation of all the data points of the dynamic yarn length changes by using mathematical software. It was found that the OCV change increased proportionally with the increase in acceleration by 2%, 5%, 10%, and 20% strain deformations for 0.1 s (Fig. 4). The generated OCV increased with a higher applied acceleration and the changes appeared to have a linear relationship with the applied acceleration (Fig. 5).

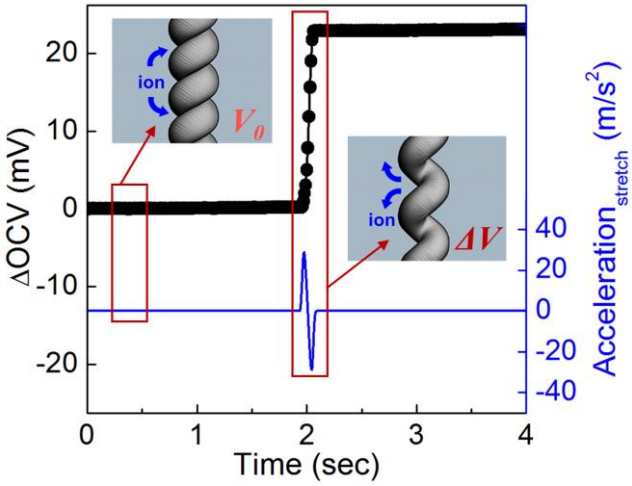

Fig. 3. Dynamic response of self-powered CNT yarn sensor and the estimated stretching acceleration for stretch-hold of CNT yarn. Inset figures represent changes in electrochemical states for releasing and stretching of coiled CNT yarn.

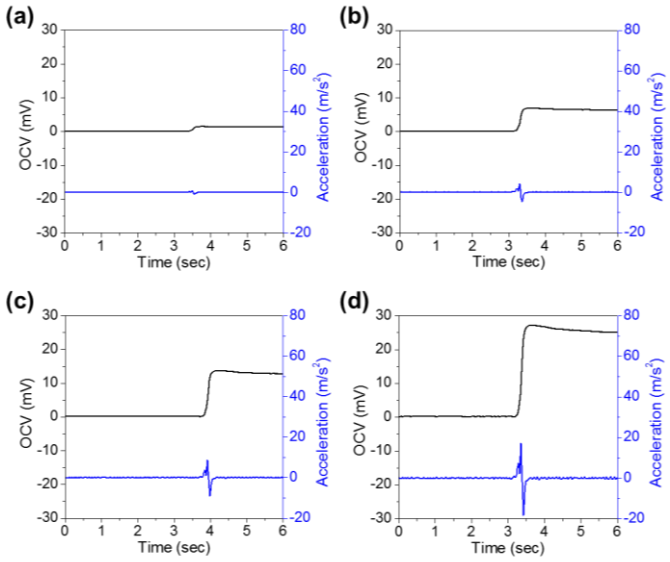

Fig. 4. Dynamic responses with OCV and the estimated stretching acceleration for stretch-hold of CNT yarn: with a) 2%, b) 5%, c) 10%, and d) 20% stretching.

The periodic acceleration sensing characteristics of the CNT yarn sensor were evaluated. An electrodynamic vibration exciter was used for periodic acceleration applied with sinusoidal tensile vibrations and one side of the CNT yarn sensor with both ends tethered was directly connected to the exciter (Fig. 2). Fig. 6(a) shows the dynamic response of the CNT yarn acceleration sensor to strain deformations at 10 Hz stretching. This sinusoidal variation in OCV increased with increasing the strain from 5% to 30%. Although OCV baselines were slightly different with test conditions, we considered the amount of OCV changes as a sensing signal. Fig. 6(b) represents the correlation with the generated maximum OCV, the applied strain, and the evaluated maximum acceleration. The OCV change was linearly proportional to the strain deformations and the corresponding acceleration.

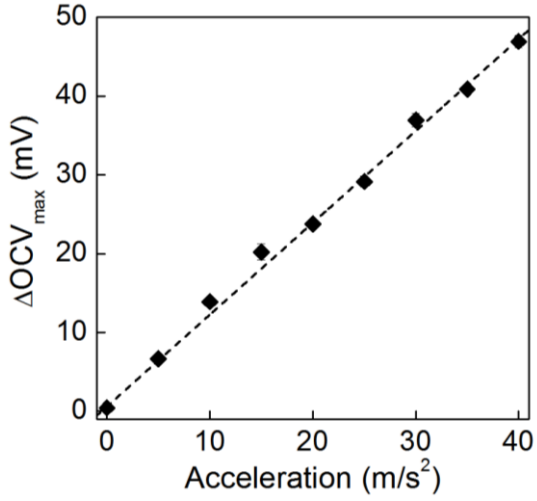

Fig. 5. Generated OCV changes for the applied accelerations with stretching of CNT yarn. Data points are the average values and standard deviations of 5 experiments.

Moreover, the coiled CNT yarn sensor could discriminate the frequency variation by using the OCV change rate (Fig. 7(a)). The OCV change rate (ΔOCV rate, V/s) can be defined as the dynamic sensor response to CNT yarn stretching (Fig. 7(b)). The OCV change rate increased as the applied frequency was increased from 0.128 to 1.890 V/s, which means that frequency detection is possible. Fig. 8(a) represents the variation of sensitivity at various frequencies. The sensitivity (Vs^{-1}/ms^{-2}), which means a sensor signal per acceleration, was defined as the slope in the acceleration–OCV rate plot (Fig. 8(b)). Acceleration levels were controlled by the applied strains at the specific frequency. As a result, the calculated sensitivity was nearly constant with the frequency variation (Fig. 8(a)).

The sensing characteristics of the CNT yarn sensor and the commercial accelerometer (model 8315A2D0, Kistler^{TM}) were evaluated and compared for controlling frequency in a periodic acceleration system. The acceleration sensing performance of a CNT yarn and commercial sensors for frequency vibrations from 1 to 20 Hz is shown in Fig. 9. Fig. 9(a)-(c) indicates that both the CNT yarn (black line) and the commercial sensors (blue line) had good dynamic responses (sinusoidal wave output) at 1, 3, and 5 Hz (< 10 Hz). However, at 10 and 20 Hz, the CNT yarn still appeared to have a sinusoidal output,

whereas the commercial sensor showed a saturated output (Fig. 9(d),(e)). The applied accelerations such as the sinusoidal vibration, which are dependent on frequency, inevitably increase at a higher frequency level in a periodic acceleration system.

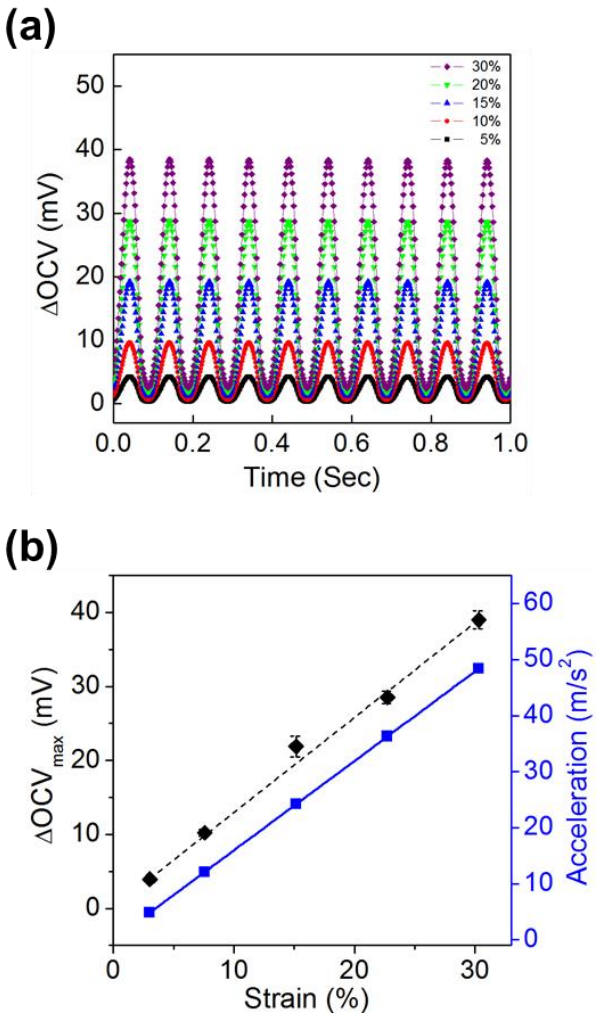

Fig. 6. Periodic acceleration sensing characteristics of CNT yarn sensors. (a) Dynamic OCV changes for sinusoidal tensile acceleration with different strain at 10 Hz. Data points are the average values and standard deviations of 10 experiments. (b) Correlated plot with OCV changes and estimated accelerations for various applied strains.

The acceleration sensing characteristics of mass configured device systems with CNT yarn are shown in Fig. 10. A mass-spring model system was adapted for sensor design as shown in Fig. 10(a) [33]. The inertial mass is a steel cylinder with the weight of 10 g, and the coiled CNT yarn acts as a spring. One end of the mass was connected to the CNT yarn and the other end was tethered with nylon fiber. The nylon fiber was used to prevent rotation of the coiled CNT yarn and friction between the outer wall of the device and the mass by dangling of the CNT yarn; the nylon fiber additionally acts as a damper and a mechanical end-stop. The device was filled with liquid electrolyte of 0.6M NaCl aqueous solution and sealed completely.When the mass configured device was exposed to a sinusoidal vibration at 10 Hz, the sinusoidal variation in OCV increased proportionally as the applied vibration increased from 3.94 to 32.18 m/s^2 (Fig. 10(b)). The generated OCV increased for the higher applied acceleration and the OCV changes appeared to have a linear relationship with the applied acceleration (Fig. 10(c)).

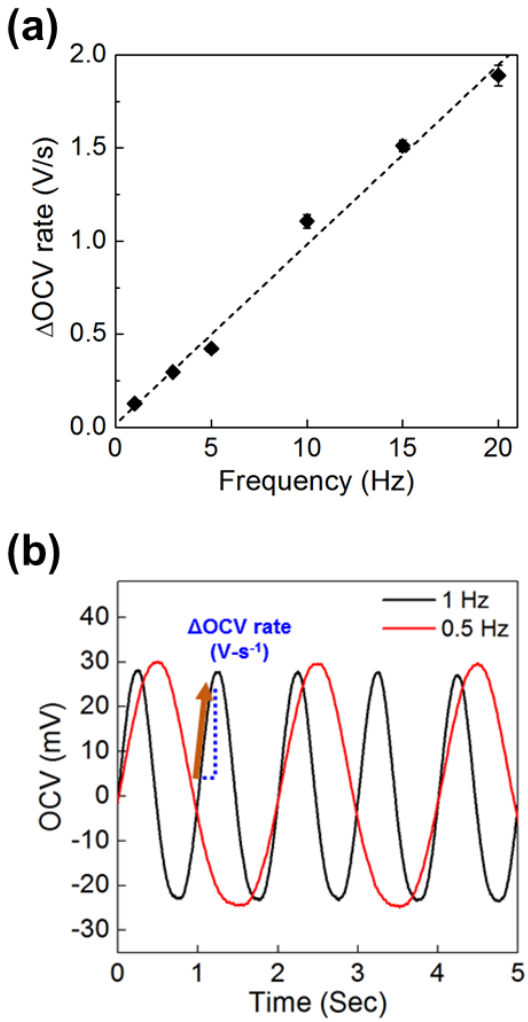

Fig. 7. Sensor responses for frequency changes in periodic acceleration system. (a) The measured OCV change rate for frequency variation with constant strain. Data points are the average values and standard deviations of 5 experiments. (b) Definition of OCV change rate (Vs^{-1}) in dynamic sensor responses for yarn stretching with 0.5 and 1.0 Hz.

However, liquid electrolyte is not suitable for practical application due to several problems, including the leak from devices, the corrosion of electric wires, and the performance degradation. Therefore, we further tested the CNT yarn acceleration sensor with solid electrolyte (10 wt% PVA/0.6M NaCl). As shown in Fig. 11(a), the mass configured device systems (as shown in Fig. 10(a)) with solid electrolyte showed the proportional sinusoidal variation in OCV to the applied vibration from 3.94 to 32.18 m/s^2. The OCV changes showed a linear relationship with the applied acceleration. For seatbelt application test in Fig. 11 (b), CNT yarn sensor with solid electrolyte also showed the acceleration sensing performances similar to liquid electrolyte. The OCV changes of CNT yarn sensor appeared fast responses/recoveries, and the generated

maximum OCV was a linear relationship with the acceleration levels measured by the reference accelerometer.

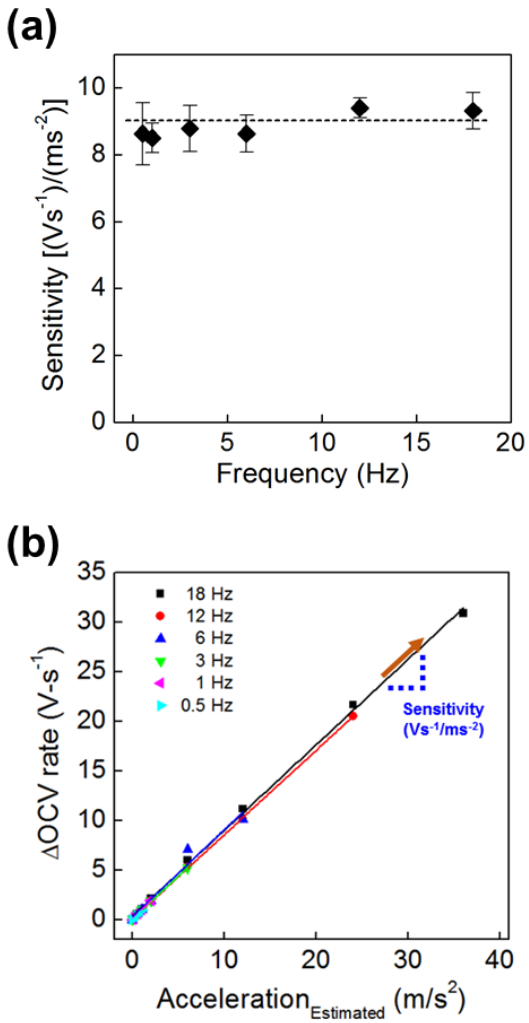

Fig. 8. Acceleration sensitivity evaluation for CNT yarn sensors. (a) Sensitivity (OCV change rate per acceleration) variation with frequency changes. Data points are the average values and standard deviations of 10 experiments. (b) OCV change rates versus estimated acceleration levels at various frequencies. The acceleration levels were controlled by the applied strains at the specific frequency. The sensitivity (Vs^{-1}/ms^{-2}) was defined as the slope in the acceleration–OCV plot.

The working principle of the self-powered CNT yarn acceleration sensor can be explained as follows (see details in Supporting Information). Once a force is applied to the yarn in the stretching direction, the yarn is accelerated, and then displacement occurs by a stretching (accelerating) force. The double integral relationship between the displacement and acceleration is given by Equation (1),

$$s(t) = \iint_0^t a(\tau)\, d\tau + v(0)t + s(0) \quad (1)$$

where $s(t)$ and $\mathrm{a}(\tau)$ are the time-dependent displacement and acceleration, and $v(0)$ and $s(0)$ denote the initial displacement and velocity, respectively. If the CNT yarn is in the stationary state initially and the acceleration is constant, then, $v(0)$ and $s(0)$ will be zero and the displacement (stretched length) will be proportional to the acceleration, $s(t) = \frac{1}{2}at^2$.

The OCV of the coiled CNT yarn depends on structural changes such as yarn diameter, bias angle, coil pitch length, and intra-bundle porosity in the harvesting sensor system. The variation of microstructure alters the number of intercalated electrolyte ions in the CNT bundles, which is closely accociated with electrochemical states of CNT yarn. Consequently, the OCV change generates from yarn length variation, is proportional to the stretched length, and also to the correlated acceleration. The theoretical sensing mechanism of the CNT yarn sensor can be explained as outlined above; however, the acceleration sensing range of a yarn-type sensor might be limited due to restrictions in the mechanical properties of yarn. A coiled CNT yarn appears to have elastic behavior, reversibly stretching and releasing without hysteresis, with a linear increase in tension (stress) during the stretching for the applied strain in the stress–strain curve [34]. The proposed CNT yarn sensor can detect quite high accelerations with fast displacement changes due to the uniform dynamic structural change characteristics of the coiled CNT yarn during the stretch–release cycles and to its robustness even at a frequency of 30 Hz [29].

The generated OCV change in CNT yarn acceleration sensor is mainly affected by the yarn length change induced by acceleration. If the yarn is stretched at a constant strain with a different frequency, the maximum OCV changes would be similar, although the stretching acceleration is different. This might be the limit of the yarn-type accelerometer, the output of which depends on yarn length change, even though this phenomenon is only confined to the sensing characteristics at periodic acceleration systems (not in irregular accelerations). However, the dependence of OCV change on yarn length could be compensated by using the OCV change rate as another sensor signal (Fig. 7(a), Fig. 8(a)).

The commercial accelerometers appeared to saturate the sensor output above 10 Hz despite the fact that their specified frequency range was 0-200 Hz (Fig. 9). This suggests that it might be difficult for these accelerometers to cover their frequency specification because their frequency range is overestimated compared with their measurable acceleration levels, and this smaller than nominal frequency range in accelerometers should be improved. The CNT yarn sensor appears to possess excellent dynamic properties with a wide frequency range of acceleration, which suggests that it is appropriate for use as an accelerometer with a fairly wide frequency range.

The proposed CNT yarn acceleration sensor has functionality for a variety of applications due to its unique and compact yarn-type design. The excellent acceleration sensing performance of the CNT yarn sensor attached to a mass suggests that the proposed CNT yarn sensors have many potential applications for acceleration detection in fabric or textile-type accelerometers in seatbelts or car seats.

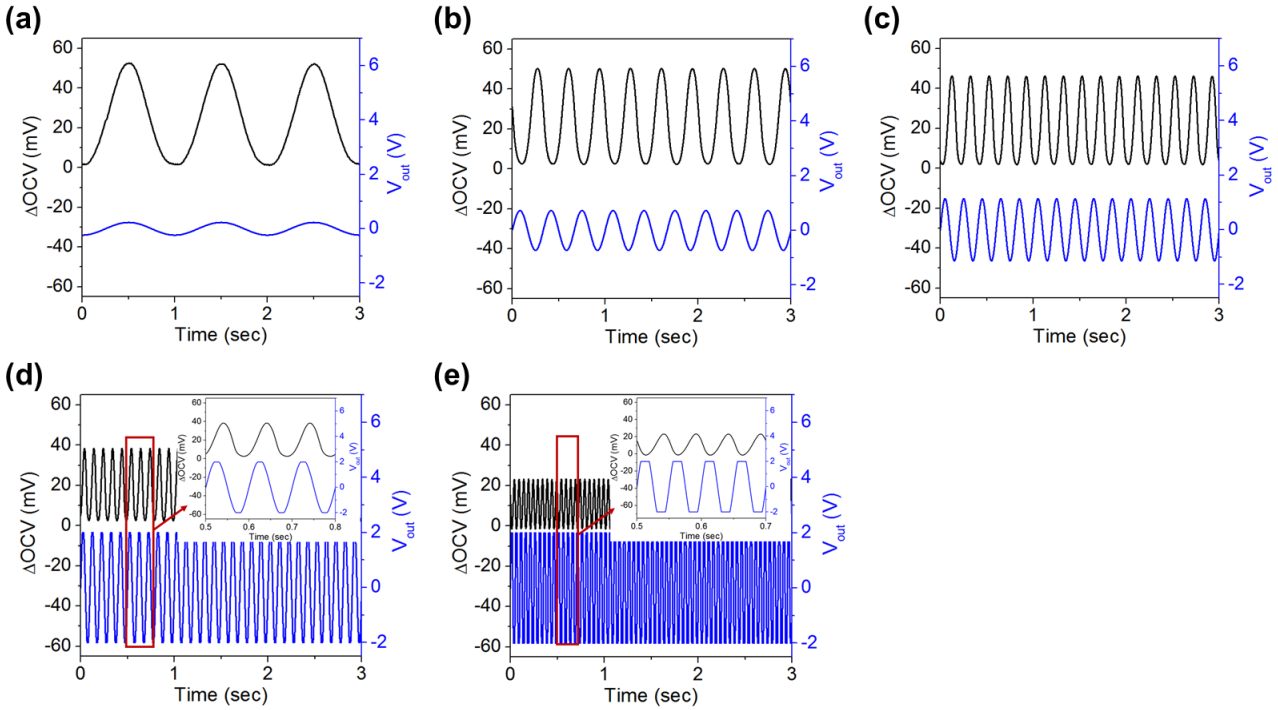

Fig. 9. Acceleration sensing performance of CNT yarn and commercial sensors for differnt frequency vibrations. Acceleration sensing characteristics at (a) 1 Hz, (b) 3 Hz, (c) 5 Hz, (d) 10 Hz, and (e) 20 Hz. Black and blue lines designate the CNT yarn sensor and the commercial accelerometer, respectively.

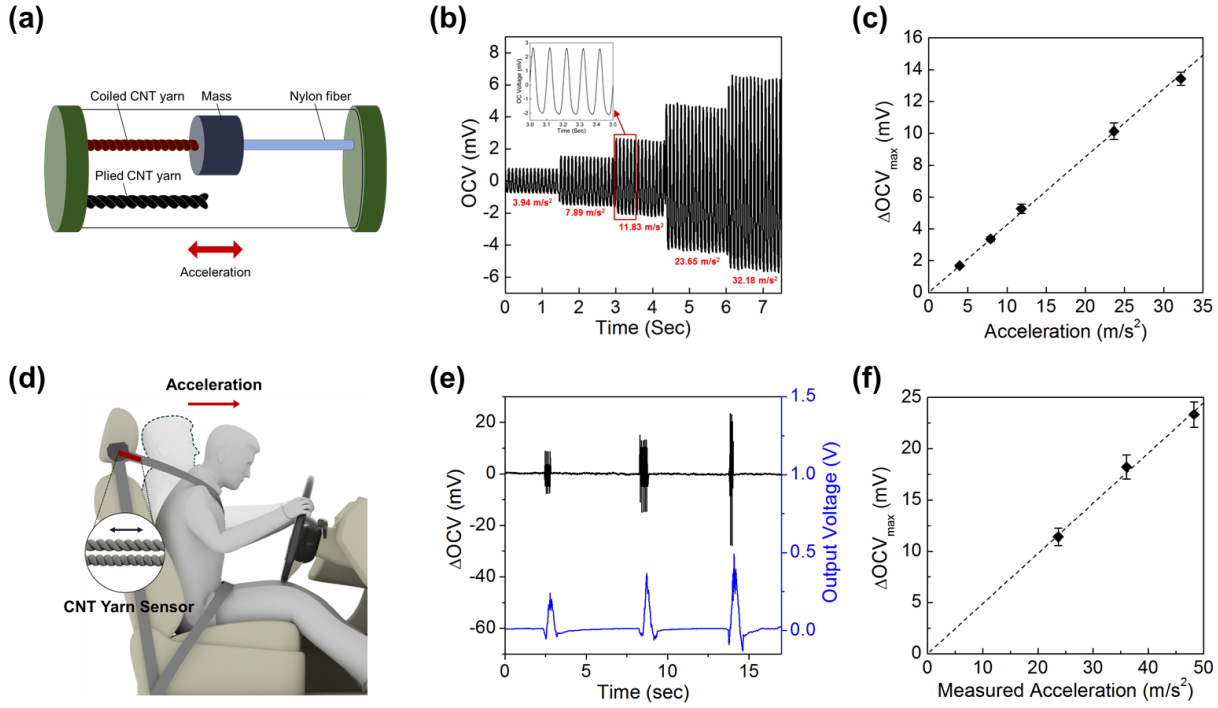

Fig. 10. Devices with CNT yarn and acceleration sensing characteristics configured with a mass load. (a–c) Device configured with a mass load and acceleration sensing characteristics; (d–f) acceleration sensing using body mass for seatbelt sensors. (a) CNT yarn sensor device configured with a mass load. (b) Dynamic OCV responses for various sinusoidal accelerations at 10 Hz. Inset figure: enlarged sinusoidal OCV waveform at an acceleration of 11.83 m/s^2. (c) Linear relationship of generated OCV changes versus applied accelerations. Data points are the average values and standard deviations of 10 experiments. (d) Illustration of acceleration sensing system for seatbelt application using body mass. (e) Dynamic OCV responses for randomly applied acceleration. The applied accelerations were controlled by varying the braking intensity. (f) Generated maximum OCV versus the measured acceleration with reference accelerometer. Data points are the average values and standard deviations of 5 experiments.

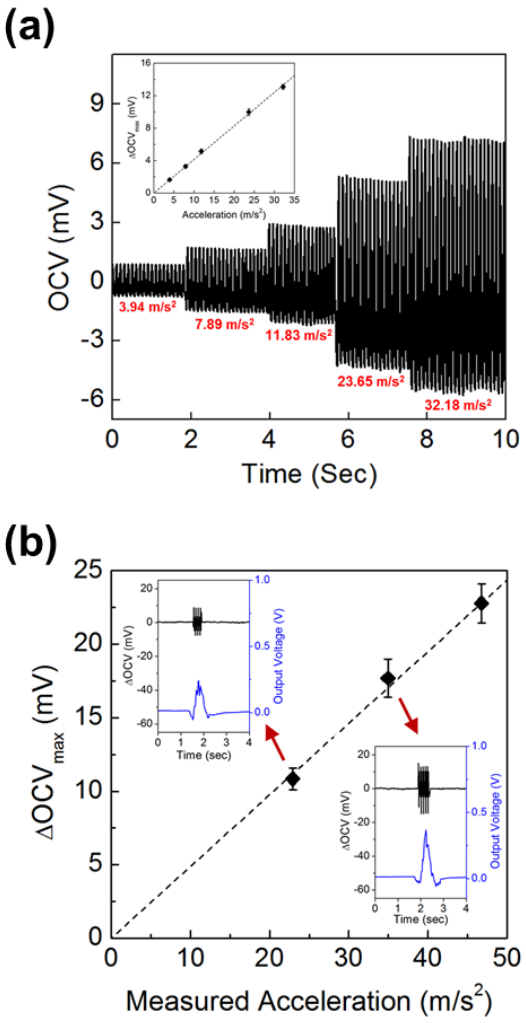

Fig. 11. Acceleration sensing characteristics mass load configured devices with solid electrolyte (10 wt% PVA/0.6M NaCl) and CNT yarns. (a) Dynamic OCV responses for various sinusoidal accelerations at 10 Hz. Inset figure is the linear relationship of generated OCV changes versus applied accelerations. Data points are the average values and standard deviations of 10 experiments. (b) Generated maximum OCV versus the measured acceleration with reference accelerometer. Inset figure is dynamic OCV responses for randomly applied acceleration. Data points are the average values and standard deviations of 5 experiment results.

V. Conclusion

We have developed and characterized a self-powered CNT yarn sensor as a novel accelerometer. The CNT yarn showed an excellent dynamic response for acceleration changes, and the change in the OCV was linearly proportional to the applied acceleration. In particular, the CNT yarn exhibited excellent acceleration sensing performance at the low frequency range (0-20 Hz), whereas the output voltage of commercial accelerometers was easily saturated at 10 and 20 Hz. In two applied models using mass configured CNT yarn devices, we showed that the OCV changes based on CNT yarn appeared to have a linear relationship with applied accelerations. Therefore, the proposed CNT yarn acceleration sensor could be further developed for practical applications such as seatbelts and car seats with fabric and textile due to its excellent sensing performance and variety of application possibilities.

References

[1] S. Lee, A. Reuveny, J. Reeder, S. Lee, H. Jin, Q. Liu, T. Yokota, T. Sekitani, T. Isoyama, and Y. Abe, "A transparent bending-insensitive pressure sensor," *Nature Nanotechnology*, vol. 11, no. 5, pp. 472, 2016.

[2] C. M. Boutry, A. Nguyen, Q. O. Lawal, A. Chortos, S. Rondeau-Gagné, and Z. Bao, "A sensitive and biodegradable pressure sensor array for cardiovascular monitoring," *Advanced Materials*, vol. 27, no. 43, pp. 6954-6961, 2015.

[3] G. Li, Z. Li, C. Wang, Y. Hao, T. Li, D. Zhang, and G. Wu, "Design and fabrication of a highly symmetrical capacitive triaxial accelerometer," *Journal of Micromechanics and Microengineering*, vol. 11, no. 1, pp. 48, 2001.

[4] Z. Gao, and D. Zhang, "Design, analysis and fabrication of a multidimensional acceleration sensor based on fully decoupled compliant parallel mechanism," *Sensors and actuators A: physical*, vol. 163, no. 1, pp. 418-427, 2010.

[5] J. Lee, H. Kwon, J. Seo, S. Shin, J. H. Koo, C. Pang, S. Son, J. H. Kim, Y. H. Jang, and D. E. Kim, "Conductive fiber-based ultrasensitive textile pressure sensor for wearable electronics," *Advanced materials*, vol. 27, no. 15, pp. 2433-2439, 2015.

[6] G. MacDonald, "A review of low cost accelerometers for vehicle dynamics," *Sensors and Actuators A: Physical*, vol. 21, no. 1-3, pp. 303-307, 1990.

[7] K. H. Kim, J. S. Ko, Y.-H. Cho, K. Lee, B. M. Kwak, and K. Park, "A skew-symmetric cantilever accelerometer for automotive airbag applications," *Sensors and Actuators A: Physical*, vol. 50, no. 1-2, pp. 121-126, 1995.

[8] A. L. Roy, H. Sarkar, A. Dutta, and T. K. Bhattacharyya, "A high precision SOI MEMS–CMOS±4g piezoresistive accelerometer," *Sensors and Actuators A: Physical*, vol. 210, pp. 77-85, 2014.

[9] A. Gesing, F. Alves, S. Paul, and J. Cordioli, "On the design of a MEMS piezoelectric accelerometer coupled to the middle ear as an implantable sensor for hearing devices," *Scientific Reports*, vol. 8, no. 1, pp. 3920, 2018.

[10] N. Luo, W. Dai, C. Li, Z. Zhou, L. Lu, C. C. Poon, S. C. Chen, Y. Zhang, and N. Zhao, "Flexible piezoresistive sensor patch enabling ultralow power cuffless blood pressure measurement," *Advanced Functional Materials*, vol. 26, no. 8, pp. 1178-1187, 2016.

[11] B. Tian, H. Liu, N. Yang, Y. Zhao, and Z. Jiang, "Design of a piezoelectric accelerometer with high sensitivity and low transverse effect," *Sensors*, vol. 16, no. 10, pp. 1587, 2016.

[12] X. Gong, C.-T. Chen, W.-J. Wu, and W.-H. Liao, "A high sensitivity piezoelectric MEMS accelerometer based on aerosol deposition method." *Proc. SPIE 10970, Sensors and Smart Structures Technologies for Civil, Mechanical, and Aerospace Systems*, p. 1097026, 2019.

[13] Q. Jing, Y. Xie, G. Zhu, R. P. Han, and Z. L. Wang, "Self-powered thin-film motion vector sensor," *Nature Communications*, vol. 6, pp. 8031, 2015.

[14] C. Xiang, C. Liu, C. Hao, Z. Wang, L. Che, and X. Zhou, "A self-powered acceleration sensor with flexible materials based on triboelectric effect," *Nano energy*, vol. 31, pp. 469-477, 2017.

[15] H. Yu, X. He, W. Ding, Y. Hu, D. Yang, S. Lu, C. Wu, H. Zou, R. Liu, and C. Lu, "A Self-Powered Dynamic Displacement Monitoring System Based on Triboelectric Accelerometer," *Advanced Energy Materials*, vol. 7, no. 19, pp. 1700565, 2017.

[16] X. Zhao, G. Wei, X. Li, Y. Qin, D. Xu, W. Tang, H. Yin, X. Wei, and L. Jia, "Self-powered triboelectric nano vibration accelerometer based wireless sensor system for railway state health monitoring," *Nano Energy*, vol. 34, pp. 549-555, 2017.

[17] Z. Su, H. Wu, H. Chen, H. Guo, X. Cheng, Y. Song, X. Chen, and H. Zhang, "Digitalized self-powered strain gauge for static and dynamic measurement," *Nano Energy*, vol. 42, pp. 129-137, 2017.

[18] W. Yang, J. Chen, Q. Jing, J. Yang, X. Wen, Y. Su, G. Zhu, P. Bai, and Z. L. Wang, "3D stack integrated triboelectric nanogenerator for harvesting vibration energy," *Advanced Functional Materials*, vol. 24, no. 26, pp. 4090-4096, 2014.

[19] B. Zhang, L. Zhang, W. Deng, L. Jin, F. Chun, H. Pan, B. Gu, H. Zhang, Z. Lv, and W. Yang, "Self-powered acceleration sensor based on liquid metal triboelectric nanogenerator for vibration monitoring," *ACS nano*, vol. 11, no. 7, pp. 7440-7446, 2017.

[20] J. Foroughi, G. M. Spinks, G. G. Wallace, J. Oh, M. E. Kozlov, S. Fang, T. Mirfakhrai, J. D. Madden, M. K. Shin, and S. J. Kim, "Torsional carbon nanotube artificial muscles," *Science,* vol. 334, no. 6055, pp. 494-497, 2011.

[21] H. Zhao, Y. Zhang, P. D. Bradford, Q. Zhou, Q. Jia, F.-G. Yuan, and Y. Zhu, "Carbon nanotube yarn strain sensors," *Nanotechnology,* vol. 21, no. 30, pp. 305502, 2010.

[22] Y. Jang, S. M. Kim, G. M. Spinks, and S. J. Kim, "Carbon nanotube yarn for fiber-shaped electrical sensors, actuators, and energy storage for smart systems twistable and stretchable sandwich structured fiber for wearable sensors and supercapacitors," *Advanced Materials,* pp. 1902670, 2019.

[23] C. Choi, J. M. Lee, S. H. Kim, S. J. Kim, J. Di, and R. H. Baughman, "Twistable and stretchable sandwich structured fiber for wearable sensors and supercapacitors," *Nano letters,* vol. 16, no. 12, pp. 7677-7684, 2016.

[24] S. H. Kim, C. H. Kwon, K. Park, T. J. Mun, X. Lepró, R. H. Baughman, G. M. Spinks, and S. J. Kim, "Bio-inspired, moisture-powered hybrid carbon nanotube yarn muscles," *Scientific reports,* vol. 6, pp. 23016, 2016.

[25] J. Lee, S. Ko, C. H. Kwon, M. D. Lima, R. H. Baughman, and S. J. Kim, "Carbon Nanotube Yarn-Based Glucose Sensing Artificial Muscle," *Small*, vol. 12, no. 15, pp. 2085-2091, 2016.

[26] K. Chen, W. Gao, S. Emaminejad, D. Kiriya, H. Ota, H. Y. Y. Nyein, K. Takei, and A. Javey, "Printed carbon nanotube electronics and sensor systems," *Advanced Materials,* vol. 28, no. 22, pp. 4397-4414, 2016.

[27] C. Yeom, K. Chen, D. Kiriya, Z. Yu, G. Cho, and A. Javey, "Large-area compliant tactile sensors using printed carbon nanotube active-matrix backplanes," *Advanced Materials,* vol. 27, no. 9, pp. 1561-1566, 2015.

[28] Y. Jang, S. M. Kim, K. J. Kim, H. J. Sim, B. J. Kim, J. W. Park, R. H. Baughman, A. Ruhparwar, S. J. Kim, "Self-powered coiled carbon-nanotube yarn sensor for gastric electronics," *ACS Sensors*, vol. 4, pp. 2893-2899, 2019.

[29] S. H. Kim, C. S. Haines, N. Li, K. J. Kim, T. J. Mun, C. Choi, J. Di, Y. J. Oh, J. P. Oviedo, and J. Bykova, "Harvesting electrical energy from carbon nanotube yarn twist," *Science*, vol. 357, no. 6353, pp. 773-778, 2017.

[30] J. A. Lee, N. Li, C. S. Haines, K. J. Kim, X. Lepró, R. Ovalle-Robles, S. J. Kim, and R. H. Baughman, "Electrochemically Powered, Energy-Conserving Carbon Nanotube Artificial Muscles," *Advanced Materials*, vol. 29, no. 31, pp. 1700870, 2017.

[31] H. Kim, and S. J. Kim, "High toughness of bio-inspired multistrand coiled carbon nanotube yarn," *Carbon,* vol. 131, pp. 60-65, 2018.

[32] K. J. Kim, J. S. Hyeon, H. Kim, T. J. Mun, C. S. Haines, N. Li, R. H. Baughman, and S. J. Kim, "Enhancing the Work Capacity of Electrochemical Artificial Muscles by Coiling Plies of Twist-Released Carbon Nanotube Yarns," *ACS Applied Materials & Interfaces*, 2019.

[33] Y. K. Pang, X. H. Li, M. X. Chen, C. B. Han, C. Zhang, and Z. L. Wang, "Triboelectric nanogenerators as a self-powered 3D acceleration sensor," *ACS Applied Materials & Interfaces,* vol. 7, no. 34, pp. 19076-19082, 2015.

[34] M. Zhang, K. R. Atkinson, and R. H. Baughman, "Multifunctional carbon nanotube yarns by downsizing an ancient technology," *Science*, vol. 306, no. 5700, pp. 1358-1361, 2004.

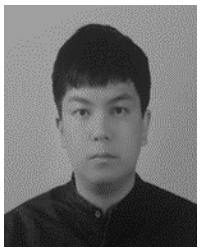

Bum-Joon Kim received a B.S., M.S and Ph.D. in the Materials Science area from University of Seoul. He is a assistant research professor in the Department of Biomedical Engineering at Hanyang University.

His current research interests include self-powered electronics such as sensors, energy harvesters and storage devices, nanomaterials synthesis and processing, nanoscale electric and optical devices, carbon based materials, and electrochemical devices.

Yongwoo Jang is a Professor in the Department of Biomedical Engineering at Hanyang University. After receiving his Ph.D. degree from Seoul National University in 2012, he continued his research as a research fellow in the Mclean Hospital of Harvard Medical School for 4 years. Currently, his scientific interests include the development of bio-hybrid intelligent artificial muscles for soft robotics, and biological applications of carbon nanotube yarn to human health monitoring and treating systems.

Ji Hwan Moon received the B.S. degrees in Department of Biomedical Engineering at Hanyang University, Korea, where he is currently working toward the Ph.D. degree in biomedical engineering.

His current research interests include the energy harvester, self-powered sensor, biosignal electrode and artificial muscle actuator based on carbon material such as carbon nanotube and graphene.

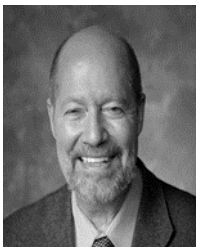

Ray H. Baughman is a Professor of Chemistry, Director of the Alan G. MacDiarmid NanoTech Institute, Robert A. Welch distinguished Chair in Chemistry. at the University of Texas in Dallas.

His current research focuses in part on developing new technologies for harvesting and storing waste energy, new types of artificial muscles, the fabrication, characterization and application of carbon nanotube sheets and yarns, sensors, new material synthesis, and fundamental structure-properties relationships for materials.

Seon Jeong Kim has worked as a Professor of Department of Biomedical Engineering at Hanyang University and Director of National Creative Research Initiative Center for Self-Powered Actuation in Korea.

His research has focused on artificial muscle as a biomimetic system, the fabrication of materials that can be driven by power sources and the investigation into artificial muscle system that can control the contraction and relaxation, and on self-powered system like sensors, energy harvesters, and storage devices.